Research Square

Preprints are preliminary reports that have not undergone peer review.
They should not be considered conclusive, used to inform clinical practice,
or referenced by the media as validated information.

Cell-Size-dependent of bacterial communities antibiotic resistome profiles and risk assessment in a river: A metagenomic analysis

Pengfei Yang
zhengzhou univerisity of light industry
Jiaxian yao
zhengzhou univerisity of light industry
Yuehua Zhang
zhengzhou univerisity of light industry
Yongzhen Zhao
zhengzhou univerisity of light industry
Zening Wang
zhengzhou univerisity of light industry
Shuhan Li
Nankai University
Fangzhou Gao
South China Normal University
Guannan Mao
Lanzhou University
Shuai Zhang
zhengzhou univerisity of light industry
Wei Hu
hvvhuwei@126.com
zhengzhou univerisity of light industry

Research Article

Keywords: Cell size, microbes, river ecosystem, antibiotic resistome, risk assessment, metagenomics

Posted Date: July 2nd, 2026

DOI: https://doi.org/10.21203/rs.3.rs-9435082/v1

License: This work is licensed under a Creative Commons Attribution 4.0 International License.
Read Full License

Additional Declarations: No competing interests reported.

Version of Record: A version of this preprint was published at BMC Microbiology on October 8th, 2026.
See the published version at https://doi.org/10.1186/s12866-026-05748-4.

Abstract

Cell size represents a critical phenotypic trait that governs microbial activity and nutrient assimilation. However, whether bacteria of different sizes exhibit similar antibiotic resistome profiles and associated risks remains unclear. In this study, bacterial communities from a river ecosystem were categorized into two size fractions: small-sized bacteria (UB; 0.1–0.45 μm) and large-sized bacteria (LB; >0.45 μm); their antibiotic resistance profiles and risk levels were comparatively analyzed using metagenomics. A total of 69 antibiotic resistance genes (ARGs) subtypes belonging to 13 ARGs types were identified. The UB and LB groups showed distinct composition of ARGs, with comparable overall abundance. ARGs encoding multidrug and tetracycline resistance were dominant in the UB group. Multidrug, bacitracin and aminoglycoside resistance genes are dominant in the UB group, and 52 ARGs subtypes were uniquely detected. Additionally, the ARG-hosting microbial community structure differed significantly between the two size groups. Nonetheless, both groups demonstrated similar antimicrobial resistance risk levels. Together, these findings offer in-depth understanding of ARG distribution in river ecosystems and highlight the previously overlooked role of small-sized bacteria in the environmental antimicrobial resistance.

Introduction

Antibiotic Resistance (AR) has emerged as a major global public health challenge in the 21st century (Duan et al., 2025). The World Health Organization (WHO) identifies it among one of the top ten threats to human health worldwide (Mao et al., 2023). The extensive use of antibiotics in medicine, agriculture and animal husbandry has accelerated the spread and diffusion of antibiotic resistance genes (ARGs) across various environmental compartments (Yang et al., 2022). River ecosystems, a crucial interface between terrestrial and marine environments, play a central role in the dissemination of ARGs (Liang et al., 2020). These ecosystems function not only as important ARG repositories but also as conduits enabling their spread.

Traditionally, microbial ecology research has focused predominantly on free-living planktonic microorganisms, while neglecting the differential contributions of varying cell size microbial communities to ecosystem functioning (Xue et al., 2024). Interestingly, aquatic microbiota can be divided into multiple components based on cell size (Hu et al., 2023; Song et al., 2019). These size-structured microbial groups exhibit significant divergent physiological characteristics, ecological functions (Liu et al., 2025), and potential for horizontal gene transfer (HGT). The differences may result in distinct patterns of their involvement to the carriage and dissemination of ARGs (Hu et al., 2025).

The primary transmission mechanisms of ARGs include vertical gene transfer (VGT) and HGT (Duan et al., 2025), with HGT considered the predominant pathway (Wu et al., 2025). HGT is mediated by mobile genetic elements (MGEs), which facilitate the transfer of genetic material among diverse bacterial taxa through processes such as conjugation, transformation, and transduction (Thomas and Nielsen, 2005). ARGs are widely disseminated via MGE-mediated HGT, involving plasmids, transposons, integrons, and

insertion sequences (Li et al., 2025). Moreover, the continuous selection pressure caused by antibiotic abuse and overuse promotes the occurrence of HGT for enhanced ARG propagation (Li et al., 2025). Additionally, the identification of microbial hosts carrying ARGs is crucial in assessing the health risks associated with AR and formulating targeted strategies to mitigate the spread of drug resistance and related pathogens (Smith et al., 2023).

Despite growing attention to environmental ARGs, several key knowledge gaps exist. First, most studies analyze the microbial community as a whole entity (Ben et al., 2019; Kim et al., 2022; Li et al., 2020; Zheng et al., 2021), ignoring the possibility of unique resistance profiles influenced by different cell-size components. Second, there is limited information on quantitative assessment of the relative contributions of environmental and biological factors in driving ARG distribution across varying sized bacterial taxa (Hu et al., 2025). Third, the co-occurrence patterns of ARGs with MGEs and their potential roles in VGT and HGT are poorly understood. Lastly, a molecular framework evaluating environmental resistance risks is lacking, hindering the linkage of the detected ARG abundance in size-fractionated bacterial communities with actual ecological health risks.

This study investigates a typical river ecosystem as the research object. Using the hierarchical filtration technique, the microbial communities were classified into different components of variable cell size (0.1–0.45 μm and > 0.45 μm) (Liu et al., 2019; Wang et al., 2009, 2010; Zhang et al., 2023a; Zheng et al., 2023). Combined with high-throughput metagenomic sequencing and bioinformatics analysis, the following scientific questions were systematically addressed: (1) Do the diversity, abundance, and distribution characteristics of ARGs differ markedly among size-structured microbial communities? (2) Which environmental and biological factors govern the distribution patterns of ARGs within different components? (3) What are the similarities and differences in the association patterns of ARGs–MGEs across varied cell size components, and what implications do they hold for HGT potential? (4) How can an anti-resistance risk assessment model applicable to river ecosystems be constructed based on molecular characteristics? The results in the present study contributes three main aspects. Methodologically, it integrates cell size fractionation with metagenomics to characterize the size-dependent distribution of ARGs. Theoretically, it clarifies the association mechanism between the cell size of microbial communities and the structuring of resistance groups. From an applied perspective, it proposes a molecularly informed framework for environmental resistance risk assessment. These findings provide valuable insights into the environmental transmission of ARGs, technically support the formulation of targeted AR control strategies for river systems, and have important implications in ensuring aquatic ecosystem security and public health.

Materials and methods

Study area

Samples were obtained from a tributary near the Danjiangkou Reservoir. At each site, 5 L surface water was collected and transported to the laboratory under low temperature conditions. The sampling

locations are depicted in **Figure S1**. The geographical coordinates and physiological parameters of the mapped sites are presented in **Table S1**.

Cell sorting and sample pretreatment

Flow cytometry (FCM) was employed to determine total cell concentration (TCC) in water samples(Hu et al., 2023). Briefly, 0.5 mL of each sample was transferred into a 1.5 mL sterile centrifuge tube and incubated at 37°C for 5 min (Hu et al., 2023). Afterward, 5 μL of SYBR Green I fluorescent dye (10^{-5} diluted from the commercial stock) was introduced. Samples were then incubated in the dark for 10 min before bacterial enumeration. Threshold for the green fluorescence channel (FITC-A) was adjusted to 1000 to eliminate background noise. A size gradient filtration protocol was implemented to segregate river microbiome (Hu et al., 2024, 2022; Liu et al., 2016; Zheng et al., 2023). Water samples were initially filtered through 0.45 μm membranes to enrich large-sized bacteria (LB), and sequentially through 0.1 μm membranes to retain small-sized bacteria (UB) (Zheng et al., 2024). The enriched volume depended on sample turbidity, ranging from 100–1000 mL and 1000–1500 mL for LB and UB groups, respectively (Gao et al., 2024).

DNA extraction and sequencing

Total genomic DNA of the microbial community was extracted using the Power Water DNA isolation kit (QIAGEN GmbH, Germany), adhering to the manufacturer's instructions. DNA concentration was quantified on a Qubit®4.0 Fluorometer (Thermo, USA), ensuring sufficient yield and quality of isolated DNA. A total of 500 ng DNA per sample was used for library preparation. Concisely, A total of 500 ng of DNA from each sample was used as input material for DNA library preparation. In brief, genomic DNA was fragmented into approximately 500 bp fragments using a Covaris 220 system, followed by purification and end repair. PCR amplification was then performed using the 2× Super Canace® II High-Fidelity Mix, Primer Mix (p5/p7), and adaptor-ligated DNA. The resulting PCR products were purified using Hieff NGS™ DNA Selection Beads, and library quality was assessed with a Qubit® 4.0 Fluorometer. The libraries were then quantified and pooled for sequencing. Fastp software (v0.36) was used to evaluate the quality of the sequencing data (Chen et al., 2018). Clean reads from each sample were assembled separately using MEGAHIT to generate sample-specific assemblies (Li et al., 2015). Gene prediction was performed on the assembled contigs (> 500 bp) using MetaGeneMark (Tang and Borodovsky, 2014). Predicted genes with lengths ≥ 300 bp from all samples were pooled and clustered at ≥ 95% sequence identity and ≥ 90% coverage using CD-HIT (Limin et al., 2012). Gene abundance for a certain sample was eatimated by SOAPaligner (version 2.21) with 95% identity (Li et al., 2008). Finally, DIAMOND (version 2.0.13) was used to align the gene set against the NR, KEGG, GO and CARD databases to obtain species and functional annotations for the predicted genes (Buchfink et al., 2015).

Antibiotic resistome profiling

To identify possible ARGs, clean reads from each sample post-optimization were assembled using MEGAHIT (version 1.1.2) and contigs sequences were generated (Dinghua Li et al., 2015). For further analysis, contigs ≥ 300 bp were subsequently selected. ORFs within contigs of the assembled sequences were predicted using Prodigal (version 2.6.3) (Hyatt et al., 2010); selected ORFs ≥ 100 bp were translated into amino acid sequences. Annotation of drug-resistant genes was carried out via DeepARG (version 1.1.2) (Arango-Argoty et al., 2018). Clean reads of each sample were mapped with the nucleic acid sequences of ARG-like ORFs (Li and Durbin, 2009). The matched number of reads was counted to calculate the abundance of ARG types or subtypes. Species annotation was performed for all ARG-carrying ORFs using the BLASTp method in DIAMOND (version 2.0.15.153) (Buchfink et al., 2015). Based on previous literature, ARGs can be categorized into RankI–IV determined by their associated health risks (Li et al., 2025).

Statistical analysis

Network analyses were conducted in R using packages 'igraph', 'Hmisc' and 'qvalue'. Spearman correlation coefficients were calculated between genes, and significant correlations were selected to construct co-occurrence network maps. Gephi was adopted to visualize networks and compute topological features such as each network node (Qi et al., 2022). Composition of bacterial community and genes was assessed via principal component analysis (PCoA). Partial Mantal tests were performed to explore the effects of environmental factors on ARG profiles (Hu et al., 2024). Procrustes analysis was used to study the relationships between ARGs and bacterial taxa (Zhang et al., 2023). Partial least squares-path modeling (PLS-PM) was applied to examine the direct and indirect influence of key divers on ARG profiles in the R ‘plspm’ package (Wang et al., 2024). Significant correlations between ARG and MGE subtypes were drawn employing the R (4.1.2) Hmisc package. The differences among the abundance of ARGs, resistance mechanisms of ARGs, ARG-MGE co-occurrence types were tested by Wilcox rank-sum test, which were adjusted by FDR.

Results

Concentration and cell size of UB and LB groups

The cell size within LB group was consistently larger than in the UB group (**Table S2**). Similarly, the TCC of UB group was lower, ranging from 1.5-4.5×10^7 cells/mL, relative to that of LB group (3.0-12.0×10^7 cells/mL) (**Table S2**). Notably, the UB group exhibited a broad concentration range across river samples, and reached levels comparable to the LB group in some samples.

ARG profiles and resistance mechanism in UB and LB groups

Total abundance of ARGs in the LB group spanned from 9.5×10^3 to 3.7×10^4 TPM, reflecting no significant difference compared with the UB group (1.8×10^4 to 3.8×10^4 TPM) (**Figure 1A, Figure S2**). However, composition of ARGs differed markedly between the two groups (**Figure 1B**). A total of 69 ARG subtypes

belonging to 13 ARG types were identified in the river samples (**Figure 1C and 1D**). Detected ARG subtypes in LB group (64 subtypes) outnumbered that in UB group (52 subtypes), with 47 shared subtypes (**Figure 1D**). All identified ARGs represented 3 key resistance mechanisms across both groups, including antibiotic efflux, target modification (inactivation, alteration, protection, and replacement), and reduced antibiotic permeability to limit uptake (**Figure 1E**). The abundance of antibiotic inactivation and target replacement presented considerable differences in UB and LB groups (**Figure 1E**). Five ARG types (multidrug, tetracycline, aminoglycoside, bacitracin, and peptide) showed significantly distinct abundance between the two groups (**Figure 1F**). Particularly, multidrug and tetracycline resistance genes were notably more abundant in the UB group (p<0.01; **Figure 1F**). The relative abundance of ARGs, namely *evgS*, *Tx*R, *optr*A, *nov*A, *efr*B, were elevated in the LB group than in the UB group. Conversely, *bas*S, *tet*B60, *bac*A, *oleC*, *ParS, mreA, tet*36, *arn*A were enriched in the UB group (**Figure 1G**).

Genetic localization of ARGs in LB and UB groups

The genetic locations of ARGs in river samples were predicted (**Figure 2A**). Overall, ARGs were predominantly located on chromosomes rather than on plasmids in both groups (p<0.001; **Figure S3**). Compared to the UB group, the LB group exhibited a lower proportion of plasmid-associated ARGs and a higher proportion of chromosomal ARGs (**Figure 2B**).

To evaluate the potential mobility of ARGs, the co-occurrence relationships of specific MGEs with ARGs were analyzed. A total of 76 MGE subtypes were identified and classified into integrases, recombinases, and transposases (**Figure 2C**), with transposase being the dominant type (**Figure 2C**). Moreover, the abundance of transposases was significantly enhanced in LB group than in UB group (p<0.05; **Figure 2C**). ARG-MGE coexistence patterns differed between the two groups (**Figure 2D**). Antibiotic efflux co-occuring with MGEs represented the primary pattern in both groups (**Figure 2D**). This pattern was more pronounced in the UB group, whereas MGE co-occurence with antibiotic target alteration and target protection was less abundant in the UB group relative to the LB group (**Figure 2E**).

Identification of ARG-harboring hosts in UB and LB groups

Microbial hosts of ARG-carrying contigs were revealed via taxonomic annotation. Phylum level analysis of microbial community composition highlighted Actinobacteria and Proteobacteria as the dominant phyla in both group (**Figure 3A and 3B**). At the genus level, *Acinetobacter*, *Teleaulax*, *Limnohabitans*, *Candidatus Planktophila* were cardinal (**Figure 3A and 3B**). PcoA analysis indicated substantial differences in ARG-hosting bacterial communities between LB and UB groups (P=0.025; **Figure 3C**). Further analysis identified *Acinetobacter johnsonii*, *Pseudomonas fluorescens*, *A. baumannii* and *A. lwoffii* as the chief pathogenic hosts in both groups (**Figure 3D**).

Assessment of ARG-associated risks

All identified ARGs were classified into four risks categories using ARG-Ranker (**Figure 4A**). Highest risk ARGs were included in Rank I, followed sequentially by Rank II, III and IV. Most ARGs detected in both UB

(96.54 %) and LB (96.22 %) groups were assigned to Rank IV, representing the lowest risk category (**Figure 4B and 4C**). Inversely, a small fraction of ARGs fell into the highest risk category Rank I (designated “current threats”), accounting for 2.05% and 1.37 % in the LB and UB groups, respectively (**Figure 4B and 4C**).

Driving factors of ARG distribution and dissemination in UB and LB hosts

Mantal and partial mantal tests were performed to further quantify the influence of physicochemical factors on ARG distribution and spread (**Table S3**). ARG profiles were primarily affected by TP in the LB group and DO in the UB group. Procrustes analysis demonstrated a significant concordance between alterations in ARG abundance and bacterial community structure (P=0.025; **Figure S4**). Mantel test analysis further revealed a strong correlation between MGEs coexisting with microbial hosts and ARG distribution as well as spread (p=0.001; **Figure S5**). Contribution analysis indicated that environmental factors (pH: 19.83%, DO: 16.55%, TP: 16.06%), MGEs (transposase: 52.15%, integrase: 27.3%) and bacterial community (Actinobacteria: 26.04%, Gammaproteobacteria: 17.81%, Betaproteobacteria: 15.65%) have significant impact on the dissemination of ARGs in the LB group. Likewise, these parameters also influenced ARG spread in the UB group: environmental factor (pH: 20.51%, TOC: 17.55%, DO: 13.58%, TP: 12.31%), MGEs (transposase: 54.09%, integrase: 24.34%) and bacterial community (Actinobacteria: 48.17%, Gammaproteobacteria: 26.50%, Betaproteobacteria: 25.32%) (**Figure 5**).

Interactions among ARGs, MGEs and bacterial taxa were established via network construction and analysis (**Figure S6**). Compared with the UB group, ARG networks in the LB group exhibited higher node number, edge number, average degree and graph density (**Table S4**), indicating greater connectivity and complexity. Besides, positive correlations among ARGs, MGEs and bacterial communities dominated in both groups, suggesting that host composition and MGEs facilitate ARG dissemination.

Partial least squares path model (PLS-PM) further elucidated the expected relationship of ARGs with key driving factors across both groups (**Figure 6**). For the LB group, bacterial community (r= 0.819, P<0.05) exerted significant impact on ARGs, while other factors showed no evident direct or indirect effects (**Figure 6A**). Contrastingly, no factors directly influenced ARGs in the UB group (**Figure 6E**). According to the standardized coefficients, non-trophic physicochemical factors, nutrients and ARG hosts were the crucial variables affecting ARG profiles in the two groups (**Figure 6C and 6G**).

Discussion

To date, few limited studies have systematically compared the ARG types hosted by small-sized and large-sized bacteria in environmental systems. Hu et al (2025) reported that ARG abundance and their host composition differed significantly between low (0.1–0.45 μm) and high (> 0.45 μm) nucleic acid-carrying microbes in marine environments (Hu et al., 2025). Similarly, Ma et al. (2019) demonstrated that small (0.2–0.45 μm) and large-sized (> 0.45 μm) microbial fractions shared 81.1% of ARG diversity in drinking water based on metagenomic analyses (Ma et al., 2019). Although previous studies have shown that the UB group exhibits lower diversity than the LB group (Hu et al., 2023; Zhang et al., 2023b), the

present study identified no notable variation in the total ARG abundance between these two groups (Fig. 1A). Nevertheless, ARG profiles were markedly divergent between LB and UB groups in the river samples, aligning with previous findings (Gao et al., 2024). These results suggest that the UB group bacteria, despite their relatively lower diversity and abundance (Song et al., 2019), can play pivotal roles as keystone taxa in microbial ecosystem processes and environmental health (Gao et al., 2024).

In this study, generalist ARG types—namely multidrug, tetracycline, aminoglycoside, and bacitracin—were relatively highly abundant in the river ecosystem, consistent with previous reports in the other environments (Dželalija et al., 2024; Yang et al., 2022; Zhang et al., 2022). Multidrug resistance genes are capable of conferring resistance to a wide range of antibiotics and can be driven by various biochemical compounds, such as heavy metals, biocides, detergents, and organic solvents (Zhang et al., 2022). Therefore, these genes are regarded as the most prominent type of ARGs in global ecosystems. Their effectiveness against broad-spectrum antibiotics is largely attributed to efflux mechanism that actively expels antibiotic peptides from the cell (Bahram et al., 2018; Duan et al., 2025). Tetracycline is one of the most extensively used antibiotics worldwide and its high environmental prevalence is likely due to drug abuse or overuse (Duan et al., 2025). Tetracycline genes have been ranked behind bacitracin, beta-lactam, polymyxin, MLS, aminoglycoside and sulfonamide in the assayed river ecosystems (Gao et al., 2024). However, findings of this study were contrasting and were in line with the patterns observed for marine environments (Hu et al., 2025).

Differences in AR profiles between LB and UB groups across river, ocean and drinking water samples indicated bacterial cell size as key determinant (Hu et al., 2025). Here, ARG composition differed considerably between the two groups likely due to variations in microbial community structures (Fig. 1B), consistent with a previous report (Hu et al., 2025). Additionally, multidrug and tetracycline resistance genes were predominant in the UB group, with significantly higher abundance compared to that in the LB group (Fig. 1F). These traits suggest that the UB group community may encompass greater proportion of bacterial species carrying the drug resistance determinants, resulting in their elevated overall abundance. These findings imply that environmental AR, especially mediated by pathogenic small-sized microorganisms, may increase the risk of treatment failure and pose a potential threat to human health; Therefore, greater attention should be directed toward understanding the roles and risks of small-sized microorganisms in various ecosystems.

The distribution and spread of ARGs are governed by multiple factors including microbial hosts, abundance of MGEs, and environmental conditions (Duan et al., 2025; Li et al., 2025; Wu et al., 2025; Yang et al., 2022; Zhang et al., 2022). Previous studies have underlined a strong association between ARGs and their hosts, emphasizing the central role of host communities in shaping ARG profiles within natural environments (Kong et al., 2022; Wang et al., 2022). Similar relationship pattern was observed in the present study (**Figure S4**), potentially arising because ARGs widely exist in bacterial communities acting as their primary hosts; therefore, shifts in bacterial taxa composition will lead to corresponding variations in ARG profiles (Han et al., 2025). Furthermore, PCoA revealed significant differences in the community structures of ARG-harboring UB and LB groups (Fig. 3C). Consequently, bacterial cell size

could critically influence microbial communities, an observation consistent with previous literature underpinning cell size as the main morphological attribute that affect microbial assemblage (Xue et al., 2024). Meanwhile, bacteria of different size fractions exhibited distinct associations with ARGs, implying size-dependent ecological roles in ARG distribution (**Figure S7**). Moreover, pathogens within the UB group harboring related ARGs should be investigated in depth. In this study, *Acinetobacter johnsonii* emerged as the dominant pathogenic microorganisms in both UB and LB groups, aligning with a previous study highlighting its role as a carrier of mobile ARGs that contribute to higher ARG diversity (Gao et al., 2024). In a similar report, *Pseudomonas alcaligenes*, *P. aeruginosa* and *Mycobacterium gordonae* were identified as primary opportunistic pathogens in the small-sized bacterial community in drinking water using metagenomic assembly strategy (Ma et al., 2019). Overall, our findings demonstrate that metagenomics is a powerful technique for monitoring environmental water safety and surveillance, owing to its ability for comprehensive and high-throughput detection of ARGs and their associated host pathogens.

Previous research has demonstrated the vital role of MGEs in facilitating ARG dissemination via HGT to acquire resistance genes among various microorganisms (Chen et al., 2019). In this study, ARG dissimilarity exhibited strong correlations with MGEs in the river system (mental r = 0.896, P = 0.001) (**Figure S5**), indicating that the widespread MGE prevalence is critical for accelerating the proliferation of ARGs in the aquatic environment (Zhou et al., 2017). MGEs—including transposases, recombinases, and integrases—are common in environmental systems as possible mediators of horizontally transfering ARGs between bacteria often via plasmids and phages (Hendriksen et al., 2019; Smith et al., 2023). Here, the abundance of transposases was higher than integrases and recombinases in UB and LB groups, with notable differences between the two groups. These results indicated that HGT-mediated ARG spread was mainly accomplished through transposition in both microbial communities. Such processes of ARG dissemination promote HGT and contribute to the evolution of antibiotic-resistant pathogens (Ellabaan et al., 2021). Nonetheless, distinct patterns of ARG–MGE co-occurrence were observed between UB and LB groups (Fig. 2D), suggesting that the influence of MGEs on ARG dynamics may vary with bacterial cell size.

ARG abundance and distribution has been associated closely with certain environmental parameters (Lu et al., 2019). Factors such as temperature, nutrients, DO, and salinity, may regulate bacterial growth and proliferation, thereby directly or indirectly affecting ARG profiles (Han et al., 2025; Wang et al., 2024). Here, pH contributed significantly to the spread of ARGs than other environmental variables in the river samples (Fig. 5), corroborating with earlier reports on the deterministic role of pH in shaping ARGs profiles (Liu et al., 2023). Additionally, DO was identified as another key factor driving ARG distribution in LB and UB groups, consistent with previous findings. Different DO levels have been associated with specific ARG profiles (Bombaywala et al., 2024), with elevated DO promoting ARG accumulation and low DO may reduce ARG abundance. Concurrently, low DO conditions can also inhibit the appearance and distribution of ARGs by impeding plasmid replication (Han et al., 2025). Since environmental factors strongly influence the microbial community structure, they are likely to cause corresponding shifts in ARG profiles within the river ecosystems (Zhou et al., 2017).

Multiple factors, including bacterial community, MGEs, and environmental parameters, can alter the distribution of ARGs. Both environmental variables and bacteria composition may exert direct and indirect impact on ARG variation, suggesting the combined role of multiple interacting factors in shaping ARG profiles and dissemination in river systems. Furthermore, PLS-PM analysis revealed that non-trophic physicochemical factors, nutrients and microbial hosts were the primary drivers of ARGs in LB and UB groups **(**Fig. 6**)**. These findings infer that ARG profiles in actual aquatic ecosystems are closely regulated by surrounding environmental conditions as well as their inherent molecular and microbiological processes.

The risks posed by drug-resistant genes to human health depend on various factors, including genetic background, host pathogenicity, and possible transfer to human pathogens. In recent years, metagenomic approaches have been increasingly applied to determine the transmission risks of drug-resistant genomes and their implications in public health. Here, we quantitatively evaluated the health risks of ARGs in LB and UB groups within river ecosystems using a framework already applied to ARG risk assessment successfully (Wu et al., 2025). A predominantly low risk (Rank IV) in the UB group was essentially identical to that in the LB group. Although the majority of ARGs may not present an immediate threat, the presence of a smaller fraction of high risk (Rank I) remains of concern and warrants attention. Importantly, the UB group contributed substantially to antimicrobial resistance (AMR) risk in the river system, as evidenced by enhanced relative abundance of certain ARG types, detection of Rank I ARGs, and identification of unique ARG subtypes only within this group.

Nevertheless, future research should prioritize broader spatial scale investigations in diverse ecosystems. Despite the hindrance, this study may provide insights into the distribution patterns and risk assessment of ARGs across bacterial size fractions, along with determining the relationship between bacterial AR functions, taxonomic composition and cell size in river environments.

Conclusion

This study provides a comparative analysis of UB and LB communities in a river ecosystem. In total, 69 ARGs subtypes belonging to 13 ARG types were identified. The composition of ARGs was distinct between UB and LB groups. Notably, ARGs encoding multidrug and tetracycline resistance were dominant in the UB group than in the LB group. Correlation analysis further revealed significant differences in ARG-hosting communities between the two groups, with pathogenic bacteria detected in both groups. Despite the lower biomass, the UB group exhibited notable AMR risk, characterized by the enrichment of several ARG types and unique subtypes, alongside the presence of high risk (Rank I) ARGs. Future studies should adopt improved pretreatment strategies and advanced microbiological techniques to better capture the ecological roles and risks associated with small sized microbiome in aquatic systems.

Declarations

Authors' contributions

PYY, JXY, YHZ: Conceived and designed the experiment. YZZ, ZNW, SHL: analysed the data, FZG, GNM, SZ: supervised the study, WH: Writing, review and editing, Funding acquisition. All authors read and approved of the final manuscript.

Data availability

All sequencing data have been submitted to the NCBI Sequence Read Archive (SRA) under accession number PRJNA1106987.

Funding

This work was supported by the Science and Technology Research Project in Henan Province (252102320216), Key Research Project of Higher Education Institutions in Henan Province (26A180028), Open Project of Key Laboratory of Agro-Forestry Environmental Processes and Ecological Regulation (AFEPER202504) and Doctoral Startup Fund of Zhengzhou University of Light Industry (2025BSJJ027).

Ethics approval and consent to participate

Not applicable.

Consent for publication

Not applicable.

Competing interests

The authors declare no competing interests.

References

1. Arango-Argoty GA, Garner E, Pruden A, Heath LS, Vikesland P. n.d. DeepARG: A deep learning approach for predicting antibiotic resistance genes from metagenomic data.
2. Bahram M, Hildebrand F, Forslund SK, Anderson JL, Soudzilovskaia NA, Bodegom PM, Bengtsson-Palme J, Anslan S, Coelho LP, Harend H, Huerta-Cepas J, Medema MH, Maltz MR, Mundra S, Olsson PA, Pent M, Põlme S, Sunagawa S, Ryberg M, Tedersoo L, Bork P. Structure and function of the global topsoil microbiome. Nature. 2018;560:233–7. https://doi.org/10.1038/s41586-018-0386-6.
3. Ben Y, Fu C, Hu M, Liu L, Wong MH, Zheng C. Human health risk assessment of antibiotic resistance associated with antibiotic residues in the environment: A review. Environ Res. 2019;169:483–93. https://doi.org/10.1016/j.envres.2018.11.040.
4. Bombaywala S, Bajaj A, Dafale NA. Deterministic effect of oxygen level variation on shaping antibiotic resistome. J Hazard Mater. 2024;465:133047.

https://doi.org/10.1016/j.jhazmat.2023.133047.

5. Buchfink B, Xie C, Huson DH. Fast and sensitive protein alignment using DIAMOND. Nat Methods. 2015;12:59–60. https://doi.org/10.1038/nmeth.3176.
6. Chen S, Zhou Y, Chen Y, Gu J, Chen S, Zhou Y, Chen Y, Gu J. fastp: an ultra-fast all-in-one FASTQ preprocessor. Bioinformatics. 2018; 34(17):i884-i890. https://doi.org/10.1093/bioinformatics/bty560
7. Chen Y, Su J-Q, Zhang J, Li P, Chen H, Zhang B, Gin KY-H, He Y. High-throughput profiling of antibiotic resistance gene dynamic in a drinking water river-reservoir system. Water Res. 2019;149:179–89. https://doi.org/10.1016/j.watres.2018.11.007.
8. Duan Y, Zhang J, Petropoulos E, Zhao J, Chen Y, Wang L, Wang X, Jia R, Wu F, Li Y. Metagenomic profiling of antibiotic resistance genes in terrestrial ecosystems across china. Ecotoxicol Environ Saf. 2025;304:119096. https://doi.org/10.1016/j.ecoenv.2025.119096.
9. Dželalija M, Fredotović Ž, Udiković-Kolić N, Kalinić H, Jozić S, Šamanić I, Ordulj M, Maravić A. Large-scale biogeographical shifts of abundance of antibiotic resistance genes and marine bacterial communities as their carriers along a trophic gradient. Int J Mol Sci. 2024;25:654. https://doi.org/10.3390/ijms25010654.
10. Ellabaan MMH, Munck C, Porse A, Imamovic L, Sommer MOA. Forecasting the dissemination of antibiotic resistance genes across bacterial genomes. Nat Commun. 2021;12:2435. https://doi.org/10.1038/s41467-021-22757-1.
11. Gao F-Z, Hu L-X, Liu Y-S, Qiao L-K, Chen Z-Y, Su J-Q, He L-Y, Bai H, Zhu Y-G, Ying G-G. Unveiling the overlooked small-sized microbiome in river ecosystems. Water Res. 2024;122302. https://doi.org/10.1016/j.watres.2024.122302.
12. Han Q, Wang Y, Shi C, Qian Y, Wang X, Wang S, Sun X, Yu Q, Li H. Urban landscape lakes with backwater hide higher antibiotic resistance risk than living water. J Hazard Mater. 2025;492:138101. https://doi.org/10.1016/j.jhazmat.2025.138101.
13. Hendriksen RS, Munk P, Njage P, Van Bunnik B, McNally L, Lukjancenko O, Röder T, Nieuwenhuijse D, Pedersen SK, Kjeldgaard J, Kaas RS, Clausen PTLC, Vogt JK, Leekitcharoenphon P, Van De Schans MGM, Zuidema T, De Roda Husman AM, Rasmussen S, Petersen B, The Global Sewage Surveillance project consortium, Bego A, Rees C, Cassar S, Coventry K, Collignon P, Allerberger F, Rahube TO, Oliveira G, Ivanov I, Vuthy Y, Sopheak T, Yost CK, Ke C, Zheng H, Baisheng L, Jiao X, Donado-Godoy P, Coulibaly KJ, Jergović M, Hrenovic J, Karpíšková R, Villacis JE, Legesse M, Eguale T, Heikinheimo A, Malania L, Nitsche A, Brinkmann A, Saba CKS, Kocsis B, Solymosi N, Thorsteinsdottir TR, Hatha AM, Alebouyeh M, Morris D, Cormican M, O'Connor L, Moran-Gilad J, Alba P, Battisti A, Shakenova Z, Kiiyukia C, Ng'eno E, Raka L, Avsejenko J, Bērziņš A, Bartkevics V, Penny C, Rajandas H, Parimannan S, Haber MV, Pal P, Jeunen G-J, Gemmell N, Fashae K, Holmstad R, Hasan R, Shakoor S, Rojas MLZ, Wasyl D, Bosevska G, Kochubovski M, Radu C, Gassama A, Radosavljevic V, Wuertz S, Zuniga-Montanez R, Tay MYF, Gavačová D, Pastuchova K, Truska P, Trkov M, Esterhuyse K, Keddy K, Cerdà-Cuéllar M, Pathirage S, Norrgren L, Örn S, Larsson DGJ, Heijden TVD, Kumburu HH, Sanneh B,

Bidjada P, Njanpop-Lafourcade B-M, Nikiema-Pessinaba SC, Levent B, Meschke JS, Beck NK, Van CD, Phuc ND, Tran DMN, Kwenda G, Tabo D, Wester AL, Cuadros-Orellana, Amid S, Cochrane C, Sicheritz-Ponten G, Schmitt T, Alvarez H, Aidara-Kane JRM, Pamp A, Lund SJ, Hald O, Woolhouse T, Koopmans M. M.P., Vigre, H., Petersen, T.N., Aarestrup, F.M., 2019. Global monitoring of antimicrobial resistance based on metagenomics analyses of urban sewage. Nat. Commun. 10, 1124. https://doi.org/10.1038/s41467-019-08853-3

14. Hu W, Zhang H, Lin X, Liu R, Bartlam M, Wang Y. Characteristics, biodiversity, and cultivation strategy of low nucleic acid content bacteria. Front Microbiol. 2022;13:900669. https://doi.org/10.3389/fmicb.2022.900669.
15. Hu W, Zheng N, Zhang Y, Bartlam M, Wang Y. Spatiotemporal dynamics of high and low nucleic acid-content bacterial communities in Chinese coastal seawater: Assembly process, co-occurrence relationship and the ecological functions. Front Microbiol. 2023;14:1219655. https://doi.org/10.3389/fmicb.2023.1219655.
16. Hu W, Zheng N, Zhang Y, Li S, Bartlam M, Wang Y. Metagenomics analysis reveals effects of salinity fluctuation on diversity and ecological functions of high and low nucleic acid content bacteria. Sci Total Environ. 2024;933:173186. https://doi.org/10.1016/j.scitotenv.2024.173186.
17. Hu W, Zhou X, Liu Y, Zhang Y, Wang Y. Effects of salinity fluctuation on antimicrobial resistance and virulence factor genes of low and high nucleic acid-content bacteria in a marine environment. Microorganisms. 2025;13:1710. https://doi.org/10.3390/microorganisms13071710.
18. Hyatt D, Chen G-L, LoCascio PF, Land ML, Larimer FW, Hauser LJ. Prodigal: Prokaryotic gene recognition and translation initiation site identification. BMC Bioinf. 2010;11:119. https://doi.org/10.1186/1471-2105-11-119.
19. Kim H, Kim M, Kim S, Lee YM, Shin SC. Characterization of antimicrobial resistance genes and virulence factor genes in an Arctic permafrost region revealed by metagenomics. Environ Pollut. 2022;294:118634. https://doi.org/10.1016/j.envpol.2021.118634.
20. Kong C, He X, Guo M, Ma S, Xu B, Tang Y. The impacts of chlorine and disinfection byproducts on antibiotic-resistant bacteria (ARB) and their conjugative transfer. Water. 2022;14:3009. https://doi.org/10.3390/w14193009.
21. Li D, Liu CM, Luo R, Kunihiko S, Tak-Wah L. MEGAHIT: an ultra-fast single-node solution for large and complex metagenomics assembly via succinct de Bruijn graph. Bioinformatics. 2015;31:1674–6.
22. Li D, Liu C-M, Luo R, Sadakane K, Lam T-W. MEGAHIT: An ultra-fast single-node solution for large and complex metagenomics assembly via succinct *de bruijn* graph. Bioinformatics. 2015;31:1674–6. https://doi.org/10.1093/bioinformatics/btv033.
23. Li H, Durbin R. Fast and accurate short read alignment with burrows–wheeler transform. Bioinformatics. 2009;25:1754–60. https://doi.org/10.1093/bioinformatics/btp324.
24. Li N, Chen X, Zhao H, Tang J, Jiang G, Li Z, Li X, Chen S, Zou S, Dong K, Xu Q. Spatial distribution and functional profile of the bacterial community in response to eutrophication in the subtropical Beibu Gulf, China. Mar Pollut Bull. 2020;161:111742. https://doi.org/10.1016/j.marpolbul.2020.111742.

25. Li R, Li Y, Kristiansen K, Wang J. SOAP: Short oligonucleotide alignment program. Bioinformatics. 2008;24:713–4. https://doi.org/10.1093/bioinformatics/btn025.
26. Li S, Liu Y, Zhang Y, Huang P, Bartlam M, Wang Y. Stereoselective behavior of naproxen chiral enantiomers in promoting horizontal transfer of antibiotic resistance genes. J Hazard Mater. 2025;489:137692. https://doi.org/10.1016/j.jhazmat.2025.137692.
27. Liang J, Mao G, Yin X, Ma L, Liu L, Bai Y, Zhang T, Qu J. Identification and quantification of bacterial genomes carrying antibiotic resistance genes and virulence factor genes for aquatic microbiological risk assessment. Water Res. 2020;168:115160. https://doi.org/10.1016/j.watres.2019.115160.
28. Limin N. Beifang, Zhu, Zhengwei, Sitao, Weizhong, 2012. CD-HIT: accelerated for clustering the next-generation sequencing data. Bioinformatics.
29. Liu J, Hao Z, Ma L, Ji Y, Bartlam M, Wang Y. Spatio-temporal variations of high and low nucleic acid content bacteria in an exorheic river. PLoS ONE. 2016;11:e0153678. https://doi.org/10.1371/journal.pone.0153678.
30. Liu J, Li B, Wang Y, Zhang G, Jiang X, Li X. Passage and community changes of filterable bacteria during microfiltration of a surface water supply. Environ Int. 2019;131:104998. https://doi.org/10.1016/j.envint.2019.104998.
31. Liu J, Zhang L, Zou H, Shi H, Wang J, Xia F, Yang Y. Cell-size-dependent responses of bacterial communities to warming in the alpine grasslands of the qinghai-tibet plateau. Global Change Biol. 2025;31:e70285. https://doi.org/10.1111/gcb.70285.
32. Liu Z, Zhao Y, Zhang B, Wang J, Zhu L, Hu B. Deterministic effect of pH on shaping soil resistome revealed by metagenomic analysis. Environ Sci Technol. 2023;57:985–96. https://doi.org/10.1021/acs.est.2c06684.
33. Lu J, Zhang Y, Wu J, Wang J, Zhang C, Lin Y. Occurrence and spatial distribution of antibiotic resistance genes in the bohai sea and yellow sea areas, china. Environ Pollut. 2019;252:450–60. https://doi.org/10.1016/j.envpol.2019.05.143.
34. Ma L, Li B, Zhang T. New insights into antibiotic resistome in drinking water and management perspectives: A metagenomic based study of small-sized microbes. Water Res. 2019;152:191–201. https://doi.org/10.1016/j.watres.2018.12.069.
35. Mao G, Ji M, Jiao N, Su J, Zhang Z, Liu K, Chen Y, Liu Y. Monsoon affects the distribution of antibiotic resistome in Tibetan glaciers. Environ Pollut. 2023;317:120809. https://doi.org/10.1016/j.envpol.2022.120809.
36. Qi Q, Hu C, Lin J, Wang X, Tang C, Dai Z, Xu J. Contamination with multiple heavy metals decreases microbial diversity and favors generalists as the keystones in microbial occurrence networks. Environ Pollut. 2022;306:119406. https://doi.org/10.1016/j.envpol.2022.119406.
37. Smith WPJ, Wucher BR, Nadell CD, Foster KR. Bacterial defences: mechanisms, evolution and antimicrobial resistance. Nat Rev Microbiol. 2023;21:519–34. https://doi.org/10.1038/s41579-023-00877-3.

38. Song Y, Wang, Yufeng, Mao G, Gao G, Wang, Yingying. Impact of planktonic low nucleic acid-content bacteria to bacterial community structure and associated ecological functions in a shallow lake. Sci Total Environ. 2019;658:868–78. https://doi.org/10.1016/j.scitotenv.2018.12.274.
39. Tang S, Borodovsky M. Ab Initio Gene Identification in Metagenomic Sequences. New York: Springer; 2014.
40. Thomas CM, Nielsen KM. Mechanisms of, and barriers to, horizontal gene transfer between bacteria. Nat Rev Microbiol. 2005;3:711–21. https://doi.org/10.1038/nrmicro1234.
41. Wang X, Han C, Lan B, Wang C, Zhu G. Antibiotic resistance genes on the qinghai-tibet plateau above an elevation of 5,000 m. Environ Sci Pollut Res. 2022;29:4508–18. https://doi.org/10.1007/s11356-021-16007-6.
42. Wang X, Qian Y, Wang Y, Wang S, Bi J, Shi C, Han Q, Wan-Yan R, Yu Q, Li H. Metagenomics reveals the potential transmission risk of resistomes from urban park environment to human. J Hazard Mater. 2024;477:135387. https://doi.org/10.1016/j.jhazmat.2024.135387.
43. Wang Y, Hammes F, Boon N, Chami M, Egli T. Isolation and characterization of low nucleic acid (LNA)-content bacteria. ISME J. 2009;3:889–902. https://doi.org/10.1038/ismej.2009.46.
44. Wang Y, Hammes F, De Roy K, Verstraete W, Boon N. Past, present and future applications of flow cytometry in aquatic microbiology. Trends Biotechnol. 2010;28:416–24. https://doi.org/10.1016/j.tibtech.2010.04.006.
45. Wu Z, Mao G, Gou Y, Ji M, Ma Q, Liu Y. Profiles and risk assessment of antibiotic resistome between qinghai-xizang plateau and polar regions. Geogr Sustain. 2025;6:100342. https://doi.org/10.1016/j.geosus.2025.100342.
46. Xue R, Stirling E, Zhao K, Wang Y, Ye S, Xu J, Ma B. Putting cell size into perspective: Soil bacterial diversity and predictive function. Geoderma. 2024;443:116804. https://doi.org/10.1016/j.geoderma.2024.116804.
47. Yang J, Xiang J, Xie Y, Yu K, Gin KY-H, Zhang B, He Y. Dynamic distribution and driving mechanisms of antibiotic resistance genes in a human-intensive watershed. Water Res. 2022;222:118841. https://doi.org/10.1016/j.watres.2022.118841.
48. Zhang H, Hu W, Liu R, Bartlam M, Wang Y. Low and high nucleic acid content bacteria play discrepant roles in response to various carbon supply modes. Environ Microbiol. 2023a;25:3703–18. https://doi.org/10.1111/1462-2920.16539.
49. Zhang H, Zhou X, Li Z, Bartlam M, Wang Y. Anthropogenic original DOM is a critical factor affecting LNA bacterial community assembly. Sci Total Environ. 2023b;902:166169. https://doi.org/10.1016/j.scitotenv.2023.166169.
50. Zhang L, Ji L, Liu X, Zhu X, Ning K, Wang Z. Linkage and driving mechanisms of antibiotic resistome in surface and ground water: Their responses to land use and seasonal variation. Water Res. 2022;215:118279. https://doi.org/10.1016/j.watres.2022.118279.
51. Zhang Z, Wu C, Di Y, Zhang J, Chai B, Zhou S. Identification and relative contributions of environmental driving factors for abundant and rare bacterial taxa to thermal stratification evolution.

Environ Res. 2023;232:116424. https://doi.org/10.1016/j.envres.2023.116424.

52. Zheng B, Liu W, Xu H, Li J, Jiang X. Occurrence and distribution of antimicrobial resistance genes in the soil of an industrial park in China: A metagenomics survey. Environ Pollut. 2021;273:116467. https://doi.org/10.1016/j.envpol.2021.116467.
53. Zheng N, Hu W, Liu Y, Li Z, Jiang Y, Bartlam M, Wang Y. Phycospheric bacteria limits the effect of nitrogen and phosphorus imbalance on diatom bloom. Sci Total Environ. 2024;935:173477. https://doi.org/10.1016/j.scitotenv.2024.173477.
54. Zheng N, Hu W, Zhou X, Liu Y, Bartlam M, Wang Y. Influence of phycospheric bacterioplankton disruption or removal on algae growth and survival. Environ Res. 2023;237:117060. https://doi.org/10.1016/j.envres.2023.117060.
55. Zhou Z-C, Zheng J, Wei Y-Y, Chen T, Dahlgren RA, Shang X, Chen H. Antibiotic resistance genes in an urban river as impacted by bacterial community and physicochemical parameters. Environ Sci Pollut Res. 2017;24:23753–62. https://doi.org/10.1007/s11356-017-0032-0.

Figures

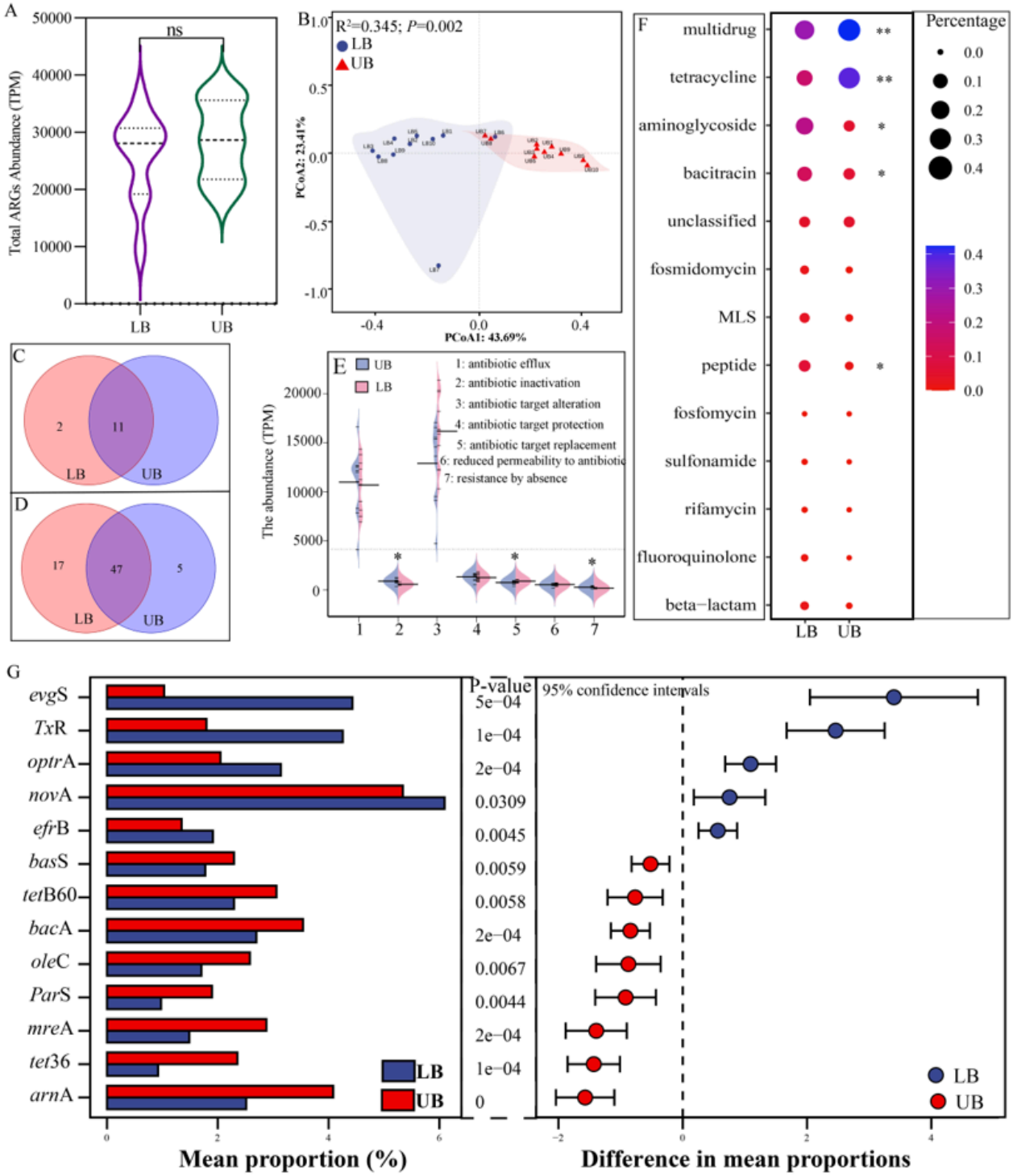


Figure 1

TPM values of ARGs between LB and UB groups (A); Principal coordinate analysis (PCoA) showing the distribution pattern of ARGs in two groups (B); The Venn diagram shows the common and unique ARGs among different groups (C: types, D: subtypes); The major resistance mechanisms of ARGs in two groups (E); the difference of ARGs type (F) and ARGs (G) in two groups. **: $p < 0.01$, *: $p < 0.05$, ns: no significant.

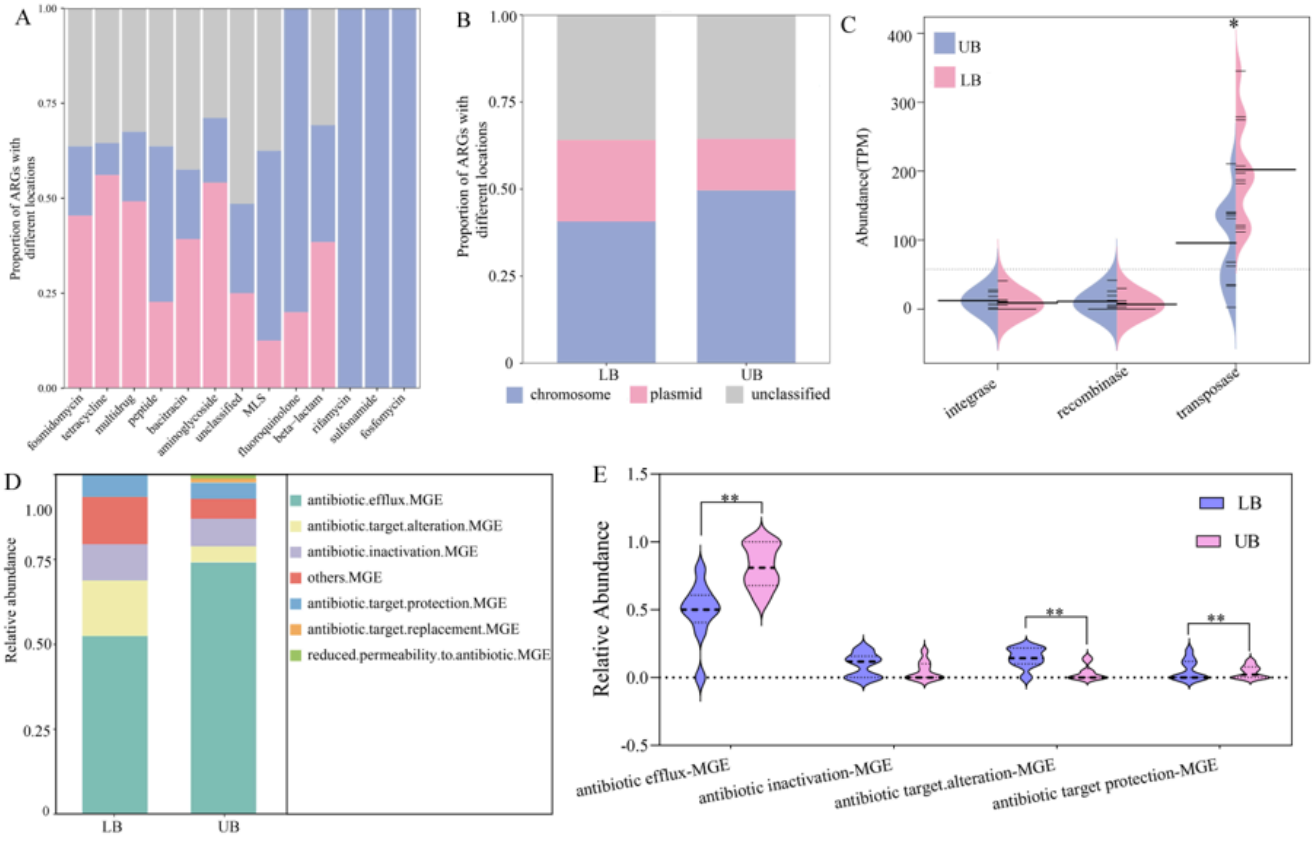


Figure 2

The proportion of ARG types located at different genetic locations (A); The proportions of ARGs classified as plasmid, chromosomal and unclassified sequences in LB and UB groups (B); The difference of the abundance of MGEs types in UB and LB groups(C); The relative abundance of the different types of ARG-MGE co-occurrence in UB and LB groups (D); And the difference of ARG-MGE co-occurrence types in UB and LB groups (E).

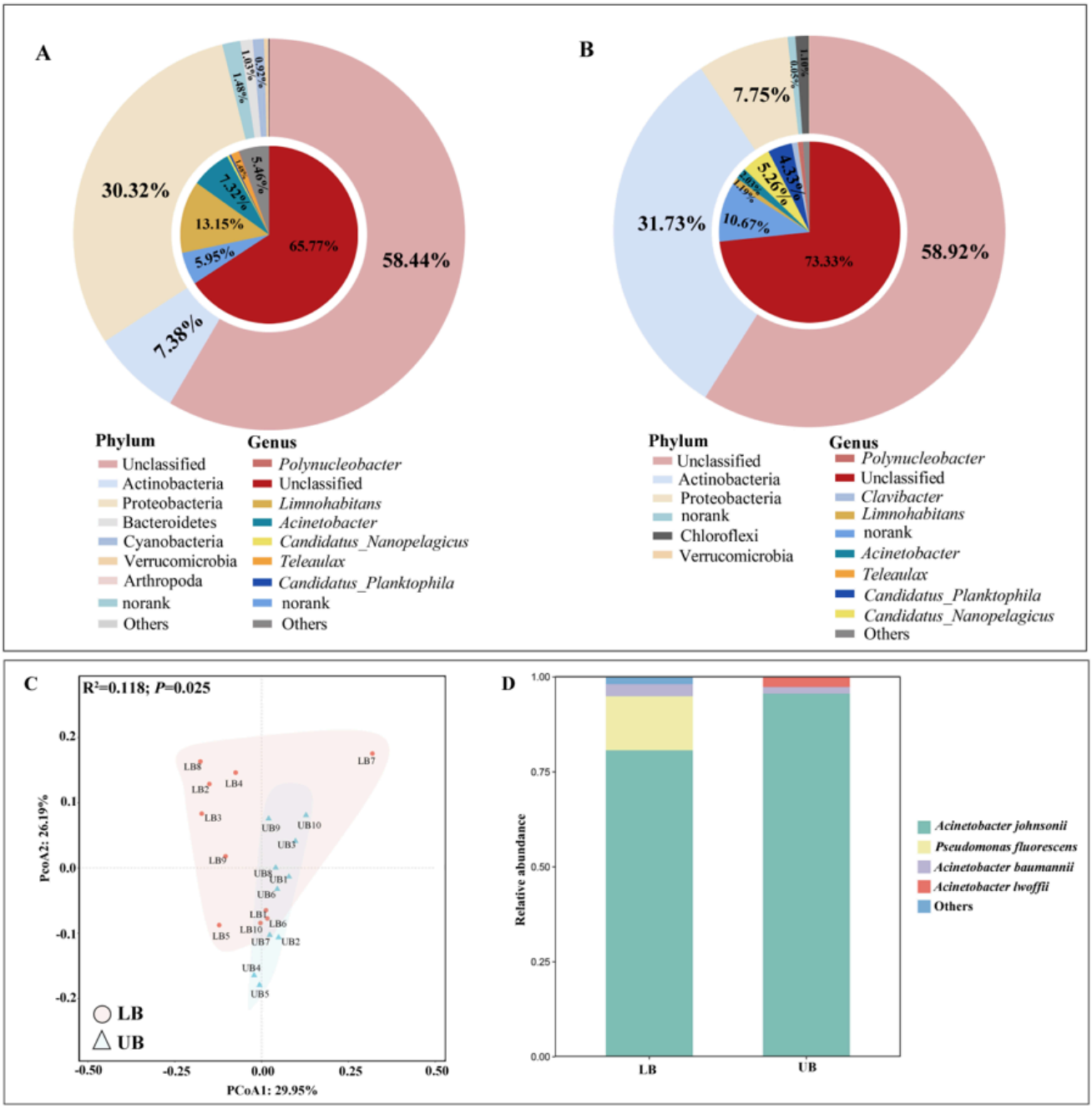


Figure 3

The community of ARGs hosts in LB (A) and UB (B) groups; Principal coordinate analysis (PCoA) showing the distribution pattern of ARGs hosts in LB and UB groups (C). The proportion of the pathogenic bacteria in LB and UB groups (D).

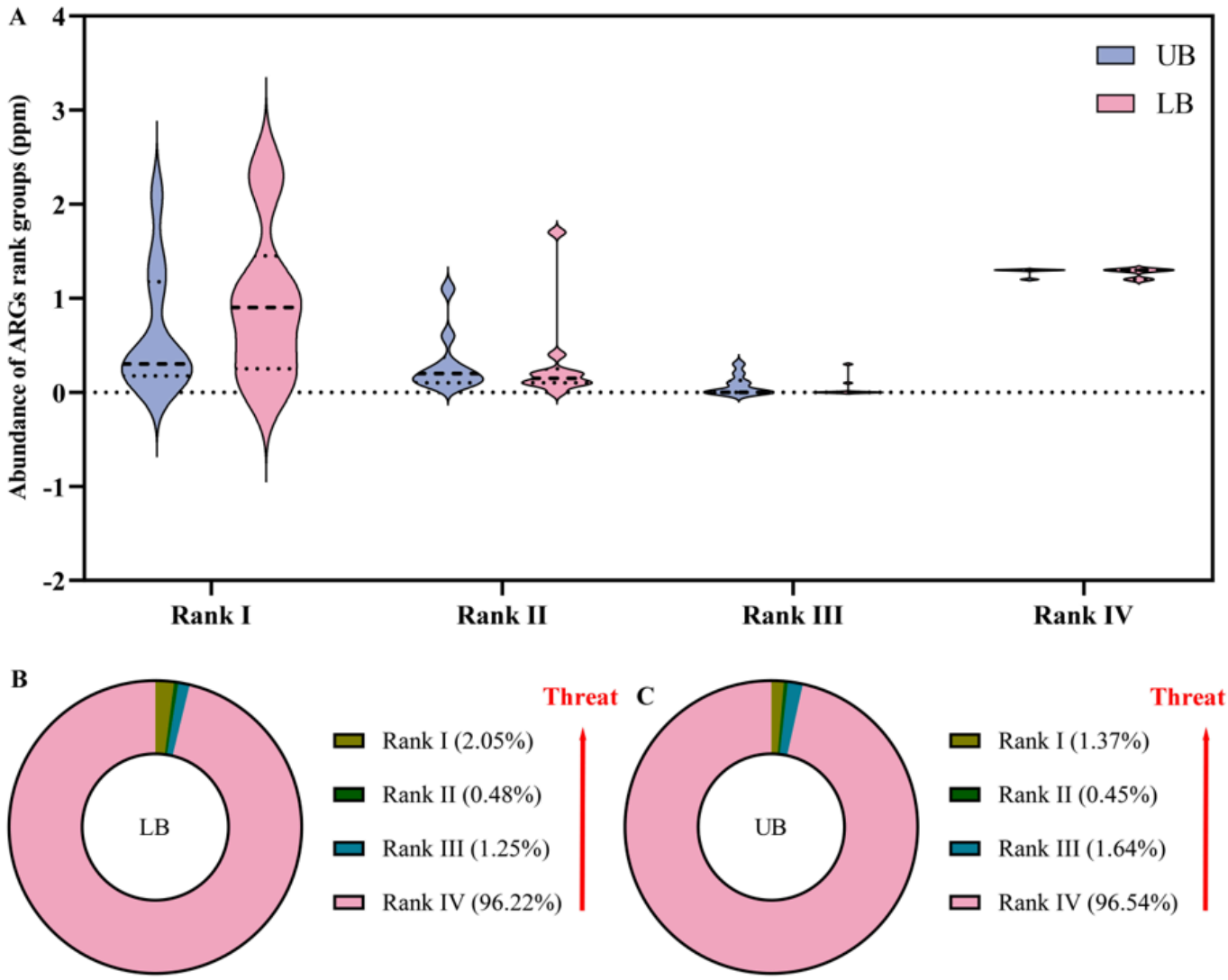


Figure 4

the risk ranks of ARG subtypes in LB and UB groups (A). and the proportion of the risk ranks in LB and UB groups (B), Risk IV–I indicates the risk ranks ranging from low to high .

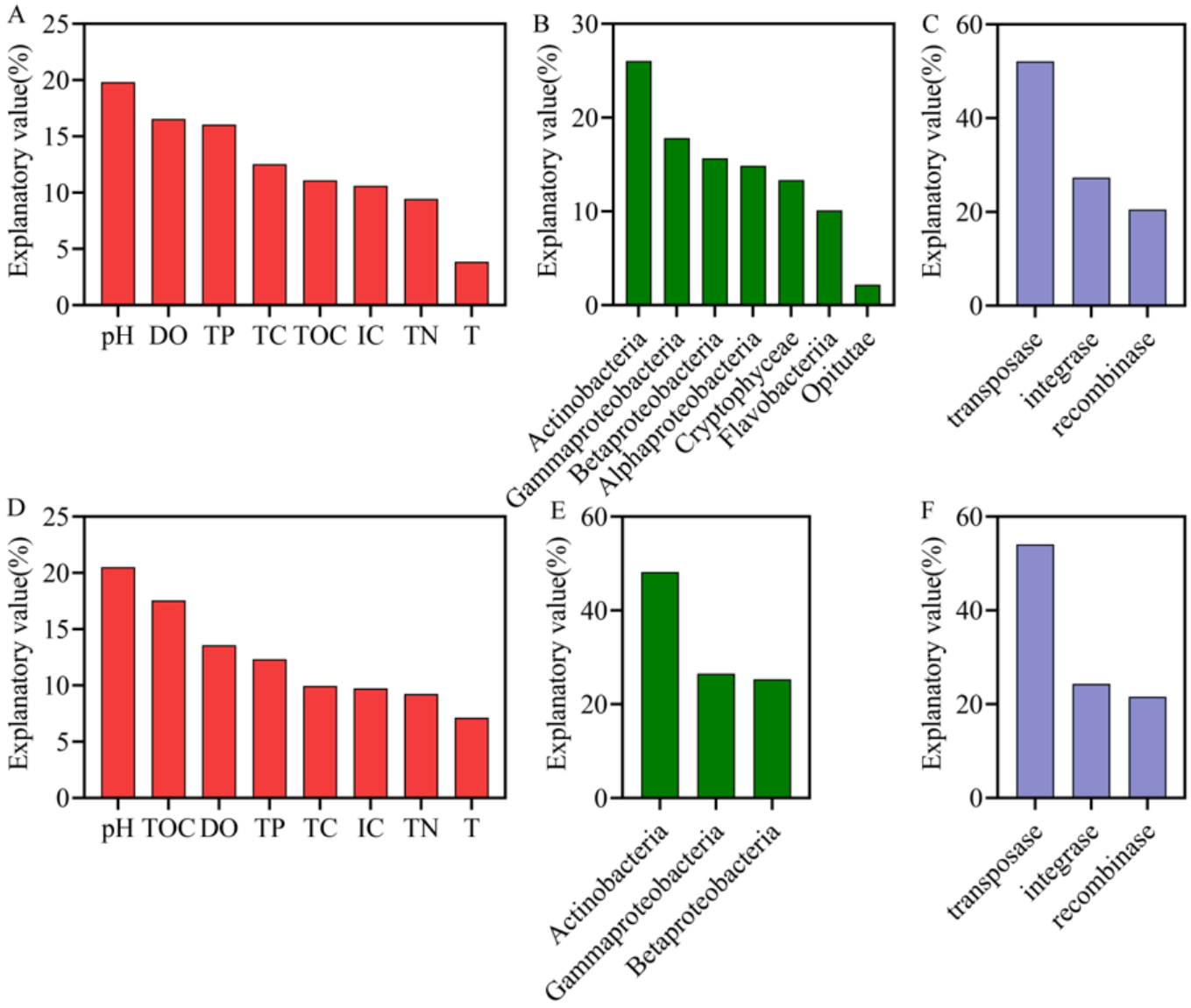


Figure 5

Contribution of environmental factors, bacterial community, MGEs to the distribution of ARGs. (A, B, C: LB, D, E. F: UB).

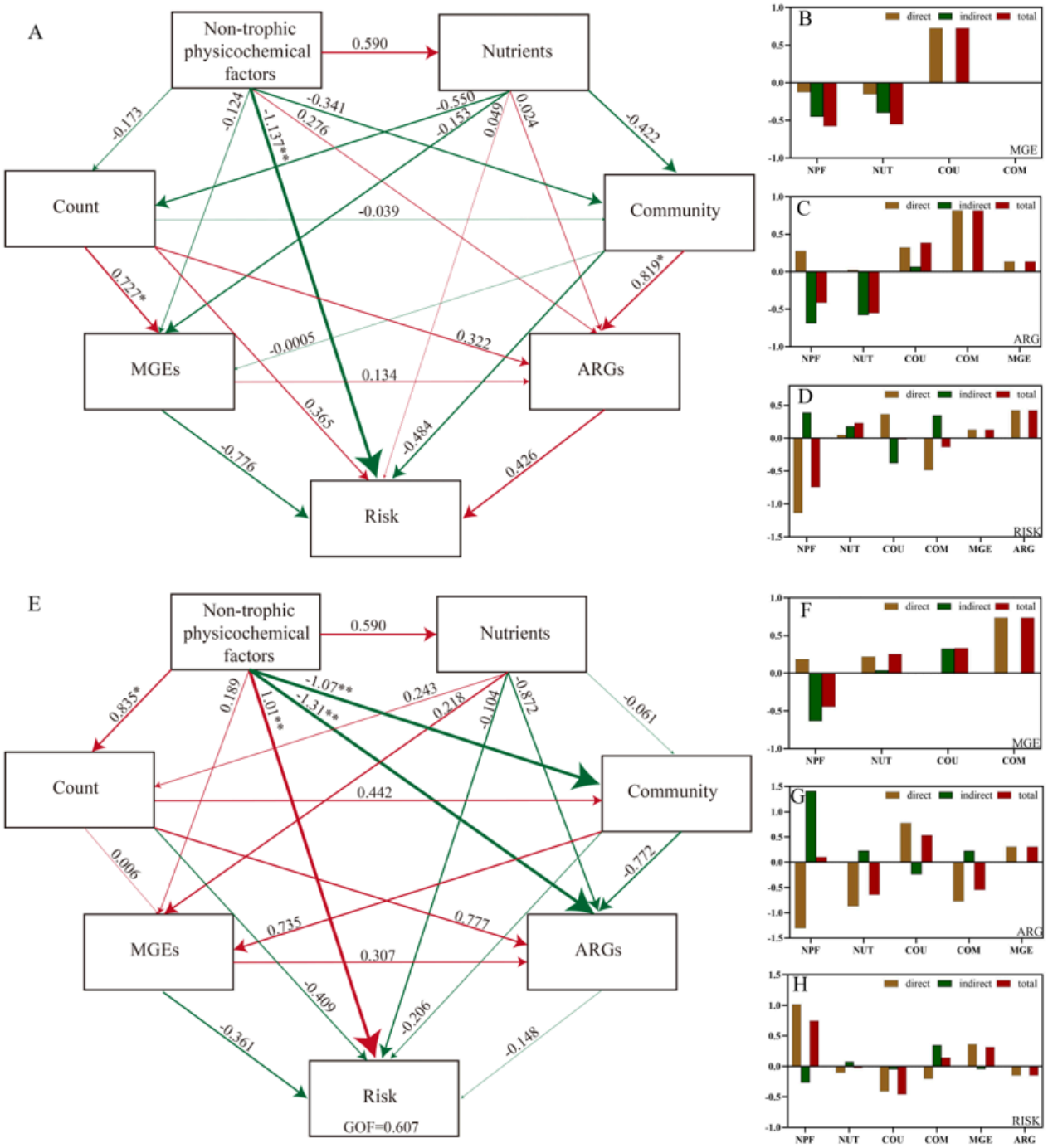


Figure 6

Driving factors of risk. The PLS-PM model was used to reveal the relationships among non-trophic physiochemical factors, nutrients, cell count, community, MGEs, ARGs and risk. Red represents positive correlation; green represents negative correlation. The thickness of the lines represents the degree of correlation. NPF = non-trophic physiochemical factors; NUT: nutrients; COU = cell count; COM = community; MGEs = MGE; ARGs = ARG. The barchart shows the effects of non-trophic physiochemical factors, nutrients, cell count, community, MGEs, ARGs on MGE (B), ARG (C) and risk (D).

Supplementary Files

This is a list of supplementary files associated with this preprint. Click to download.

- SupplementaryMaterial.docx